

Longitudinal Vortices Mixing in Three-Stream Micromixers with Two Inlets

Yi-Tun Huang, Chih-Yang Wu, Shu-Wei Huang

Abstract—In this work, we examine fluid mixing in a full three-stream mixing channel with longitudinal vortex generators (LVGs) built on the channel bottom by numerical simulation and experiment. The effects of the asymmetrical arrangement and the attack angle of the LVGs on fluid mixing are investigated. The results show that the micromixer with LVGs at a small asymmetry index (defined by the ratio of the distance from the center plane of the gap between the winglets to the center plane of the main channel to the width of the main channel) is superior to the micromixer with symmetric LVGs and that with LVGs at a large asymmetry index. The micromixer using five mixing modules of the LVGs with an attack angle between 16.5 degrees and 22.5 degrees can achieve excellent mixing over a wide range of Reynolds numbers. Here, we call a section of channel with two pairs of staggered asymmetrical LVGs a mixing module. Besides, the micromixer with LVGs at a small attack angle is more efficient than that with a larger attack angle when pressure losses are taken into account.

Keywords—Microfluidics, Mixing, Longitudinal vortex generators, Two stream interfaces.

I. INTRODUCTION

MICROMIXERS have wide applications in biochemical processes and microreactors [1]-[3]. Due to the small size of the internal structures in a microfluidic system, the flow is laminar in nature. Thus, increasing the interface between different fluids by handling fluid flows within the mixing channel is of great importance for enhancing fluid mixing. Recently, many ingenious micromixers have been developed, including active micromixers and passive micromixers [1], [2]. Active micromixers utilize moving parts or external forces to enhance fluid mixing. Passive micromixers do not require external energy except that used to drive the flows, and so the internal structures of the passive micromixers play an important role in the enhancement of fluid mixing. Although the mixing efficiency of active micromixers is better than that of passive micromixers, it is simpler to fabricate passive micromixers and easier to integrate them with microfluidic systems. Thus, passive micromixers still have been developed widely [1], [2]. Well-known examples of passive-type micromixers developed to date are the chaotic mixers [4] and split and recombine mixers [5]. Also, some research works on other designs, such as impinging [6], channel confluence [7], [8], lamination [9], hydrodynamic focusing [10], and bending, curved and/or

converging-diverging channel which induces lateral advection in the flow [11]-[14]. Besides, Bertsch et al. [15] have fabricated two passive micromixers having geometries similar to large-scale mixers and have shown that the two micromixers yield good mixing efficiency.

Longitudinal vortex generators (LVGs) are the winglets built on the channel wall to generate longitudinal vortices (LVs) behind winglets. The LVs swirl the flow around the axis parallel to the mainstream direction to enhance heat transfer in the flow. The application of LVGs has led to extensive studies of the effects of LVs on heat transfer augmentation for large-scale heat exchangers [16]. The phenomenological similarity of convective heat and mass transfer suggests that the enhancement technique for heat transfer could be adapted to that for mass transfer. Kaniewski et al. have pointed out that a LV shall be generated with an axis between the two (often parallel) streams in mass transfer configurations [17]. This is different from the manipulation of the surface layer by LVGs for heat transfer augmentation in heat exchangers. The success of the downscaling mixers presented by Bertsch et al. [15] attracts our interest in the applicability of the LVGs to mixing enhancement in microchannels. Nevertheless, there are only a few investigations considering the effects of LVs on heat transfer [18] or mixing [19] in micro-scale flows. Besides, it is found that the mixing efficiency increases without increasing the pressure applied much by the channel structure forming the sandwiched structure of streams [20]. Therefore, this paper is intended as an investigation of micromixers with pairs of rectangular winglets built on the microchannel bottom and staying with an angle of attack (θ) to the main flow direction (shown in Fig. 1) and a full three-stream (FTS) design, which allows three streams of liquids - a core stream sandwiched by two cladding streams - to flow into the mixing channel from two inlets and so to generate two interfaces between the mixing fluids at the initial stage of the mixing channel. The LVs generated by the rectangular winglets distort the two interfaces between the mixing fluids and transport the fluid to other zones of the channel which are originally occupied by the other fluid, as shown in Fig. 2. Thus, the geometric sandwiched structure of fluid streams can increase the efficiency of the LVs, and the present design of micromixers is an improvement of the original design of micromixers with only one interface between the mixing fluids at the initial stage of the mixing channel [19]. The distance from the center plane of the gap between the winglets to the center plane of the main channel (d) divided by the width of the main channel (W_m) defining the asymmetry of LVGs is found to be an important parameter for the performance of the micromixers with LVGs. The angle of

Yi-Tun Huang and Shu-Wei Huang are with the Department of Mechanical Engineering, National Cheng Kung University, Tainan, Taiwan 701, ROC (e-mail: eric10135@yahoo.com.tw, vida1152000@hotmail.com, respectively).

C.-Y. Wu is with the Department of Mechanical Engineering, National Cheng Kung University, Tainan, Taiwan 701, ROC (phone: 886-62757575-62151; fax: 886-6-2352973; e-mail: cywu@mail.ncku.edu.tw).

attack (θ) is the other notable parameter. The effects of d/W_m and θ on the performance of the present micromixers are investigated by numerical simulations. Experimental verifications are also carried out.

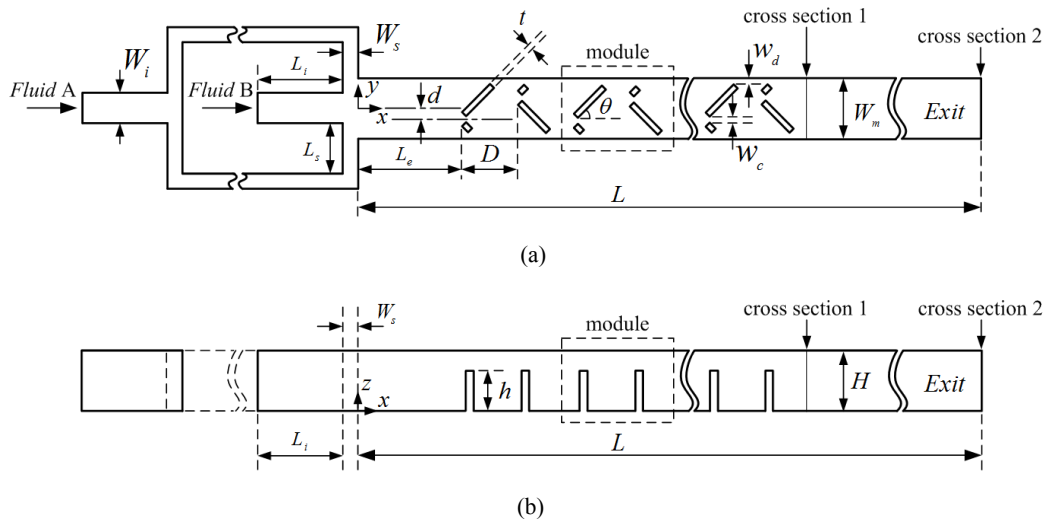


Fig. 1 Schematic diagram of the FTS micromixer with divergent RWPs: (a) top view and (b) x - z cross section at $y = 0 \mu\text{m}$

II. MICROMIXER DESIGN

The proposed FTS micromixer with rectangular winglet pairs (RWPs) mounted on the bottom of the straight main channel is shown in Fig. 1. The channel height and width are $H = 130 \mu\text{m}$ and $W_m = 3H$, respectively. The winglets with height (h) protrude into the flow at angle of attack and the winglet thickness is $t = 0.3H$. From [19], we know that the effect of the winglet spacing (D) on fluid mixing is small. In this work, we set the winglets height to be $0.75H$ and the winglet spacing to be $1.5W_m$. The fluids A and B are introduced at two inlets with channel width $W_i = 1.5H$. The inlet channel of fluid A is then split into two side inlets with equal width $W_s = 0.75H$. The inlet channel of fluid B with a length L_i of $975 \mu\text{m}$ and the two side inlets of fluid A with a length L_s of $292.5 \mu\text{m}$ are connected to the main mixing channel, and so the core stream of fluid B is sandwiched by two cladding streams of fluid A. Then, a three-stream flow with two stream interfaces is generated to double the interfacial area and the enhancement of fluid mixing can be expected. The length of the entrance channel before the first pair of LVGs built on the channel bottom is $L_e = 1300 \mu\text{m}$ and the total length of the main channel is $L = 10172.5 \mu\text{m}$. For

convenience, we call a section of channel with two staggered asymmetrical RWPs shown in Fig. 1 a mixing module. In this work, we choose the geometrical parameters, the angle of attack and the asymmetry index (d/W_m), as the influential factors to be investigated. In the mean time, we fix the values of H , W_m , W_s , W_i , t , h , D , the width of the gap between the winglets of a RWP $w_c = 32.5 \mu\text{m}$, the distance between each winglet of a RWP and its neighboring sidewall $w_d = 30 \mu\text{m}$ and the number of modules $N_m = 5$.

III. NUMERICAL SIMULATIONS

The flow and mixing in the micromixer is described by the continuity equation, the momentum equation and the species convection-diffusion equation for isothermal incompressible steady flow. The no-slip condition is set on the solid walls and the pressure at the exit is set to be 1 atm. The governing equations are solved by a commercial computational fluid dynamics code, CFD-ACE+ (CFD Research Corporation, CA, USA). The SIMPLEC algorithm is used for pressure-velocity coupling. The second-order upwind scheme with limiter is adopted for the velocity and concentration calculations.

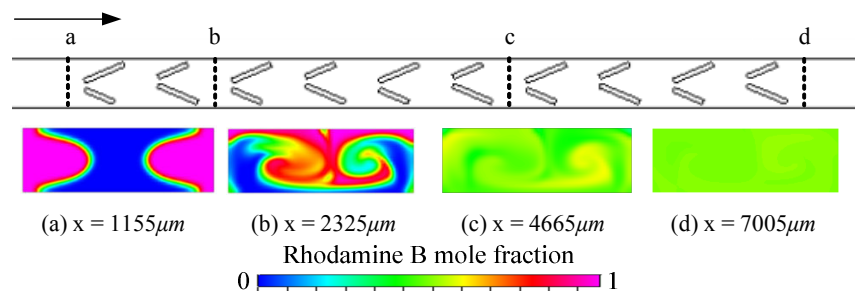


Fig. 2 Simulated concentration distributions on vertical cross sections in the downstream zone of the RWP's with $\theta = 22.5^\circ$, $h = 0.75H$, $d = 0.042W_m$ and $D = 1.5W_m$ for the case with $Re = 64$

We consider equal flow rate at both inlets, and so the mixing rate is 1:1. The fluids entering the two inlets are a $33 \mu\text{mole/l}$ solution of Rhodamine B (Fluka, Germany) in DI water and pure DI water. Due to the low concentration of the solution, the influence of fluorescent on the fluid behavior can be neglected [8]. Thus, the physical properties of water are applied to the fluid in each of the inlets in the present simulation. The density and the viscosity are 997 kg m^{-3} and $0.00097 \text{ kg m}^{-1}\text{s}^{-1}$, respectively. The diffusion coefficient of Rhodamine B in deionized (DI) water is $3.6 \times 10^{-10} \text{ m}^2 \text{ s}^{-1}$ [21]. In the present simulation, the Reynolds number is defined as $Re = \bar{u} d_h \nu^{-1}$, where \bar{u} , d_h and ν denotes the bulk flow velocity, the hydraulic diameter of the main channel and the kinematic viscosity of the fluid, respectively, and the values of the Reynolds number are selected to cover the range of flows from the diffusion domination to the convection domination of the mixing. Besides, the stopping criterion of iterative computation is that the relative residual for each variable is less than 0.0001.

To compare the mixing efficiency of micromixers with various flow conditions and geometrical parameters, the degree of mixing [22] is calculated by

$$M = 1 - \frac{\sigma}{\sigma_0} \quad (1)$$

where

$$\sigma^2 = \frac{1}{n} \sum_{i=1}^n (c_i - \bar{c})^2 \quad (2)$$

$$\sigma_0^2 = \bar{c}_0 (1 - \bar{c}_0) \quad (3)$$

Here, n denotes the total number of sampling, c_i the

concentration of Rhodamine B at a position on the cross section considered, \bar{c} the average of c_i and \bar{c}_0 the average of c_i at the beginning of the mixing process. The mixing efficiency of micromixer is represented by the value of M calculated at the exit cross section of micromixer in the following investigation.

IV. FABRICATION AND EXPERIMENTAL SETUP

The micromixers are fabricated by micro-lithography processes. Two master templates on the films of photoresist SU-8 (MicroChem, USA) for microchannel and LVG structures are fabricated by photolithography, respectively. Next, the liquid PDMS (polydimethylsiloxane; Dow Corning Corp., USA) and its curing agent are mixed in a ratio of 10:1 and poured on the SU-8 molds. After curing at 100°C for 60 min, the PDMS is peeled off from the molds. Then, the two layers of PDMS are bonded after the oxygen plasma treatment.

Before observing the mixing behaviors, we prepare the fluid flow system by filling one syringe with the solution of Rhodamine B in DI water, the other with pure DI water and connecting the two syringes to the inlets of the micromixer. And then, the two syringes are driven at the same constant flow rate by a syringe pump (KDS 220, KD Scientific, USA). Following that, we use a confocal spectral microscope imaging system (Leica TCS SP2, Leica Corp., Germany) to observe the flow and mixing in the micromixer. The images of the fluid concentration distribution on horizontal cross sections and those on vertical cross sections are acquired by scanning over the horizontal and the vertical cross sections of a mixing channel. The results of some typical examples are shown in Figs. 3 and 4.

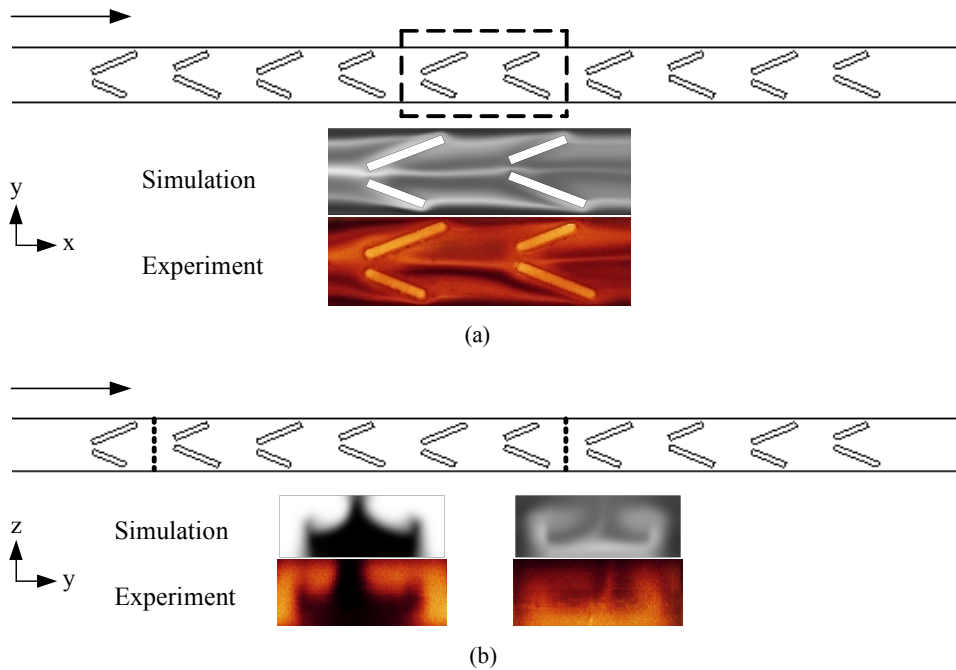


Fig. 3 Experiment (color) and simulation (gray-scale) (a) concentration distributions on the horizontal cross sections at $z = 65 \mu\text{m}$ of the third module and (b) those on the vertical cross sections at the middle plane of the first module and at the exit of the third module in a microchannel with RWPs ($\theta = 22.5^\circ$, $h = 0.75H$, $d = 0.042W_m$ and $D = 1.5W_m$) for the case with $Re = 1$

V. RESULTS AND DISCUSSION

Figs. 3 and 4 show that the concentration distributions on the horizontal mid-planes and on the vertical planes of the mixing channel obtained by simulation using structured cells with $6\mu\text{m}\times 6\mu\text{m}\times 6.5\mu\text{m}$ are in reasonable agreement with those obtained by experiment. Thus, we use the cells with such a size in following simulation.

Fig. 5 shows the flow patterns on transverse cross sections in the downstream zone of a typical example. The pressure difference at the front and back sides of the winglets generates the LVs which persist behind the winglets. It can be seen that a longer winglet generates a stronger vortex and a pair of asymmetrical winglets may generate asymmetrically counter-rotating vortices. The asymmetrical vortices stretch the contact interface between the two mixing fluids and transport the fluid to other zones of the channel which are originally occupied by the other fluid effectively, as shown in Fig. 2. Thus, the asymmetrical LVs may enhance mixing of the fluids in the

main channel.

Then, we consider the effects of the asymmetry index (d/W_m) on fluid mixing. Figs. 6 and 7 show the effects of d/W_m on the degrees of mixing and the pressure drop, respectively, of the flows in the FTS micromixer, where the divergent RWPs with $\theta = 22.5^\circ$ are built on the channel bottom. From the figures, it can be found that (i) the effects of d/W_m on the degrees of mixing is largest at a Reynolds number around 22.6, (ii) the effect of d/W_m on the pressure drop is small, and (iii) the overall performance of the mixer with $d/W_m = 0.042$ is better than that of other mixers over a wide range of Reynolds numbers. Besides, the mixing efficiency of the micromixer with symmetrical RWPs is superior to that of the micromixer with RWPs at a large asymmetry index, but inferior to that of the micromixer with RWPs at a small asymmetry index ($0 < d/W_m \leq 0.083$).

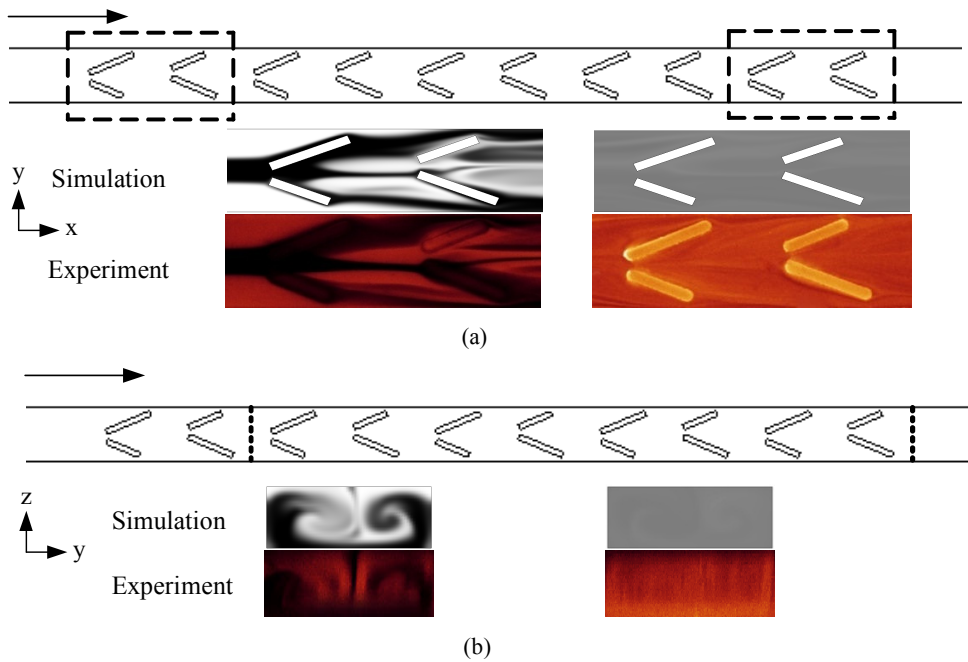


Fig. 4 Experiment (color) and simulation (gray-scale) (a) concentration distributions on the horizontal cross sections at $z = 65\mu\text{m}$ of the first and the fifth modules and (b) those on the vertical cross sections at the exits of the first and the fifth modules in a microchannel with RWPs ($\theta = 22.5^\circ$, $h = 0.75H$, $d = 0.042W_m$ and $D = 1.5W_m$) for the case with $Re = 64$

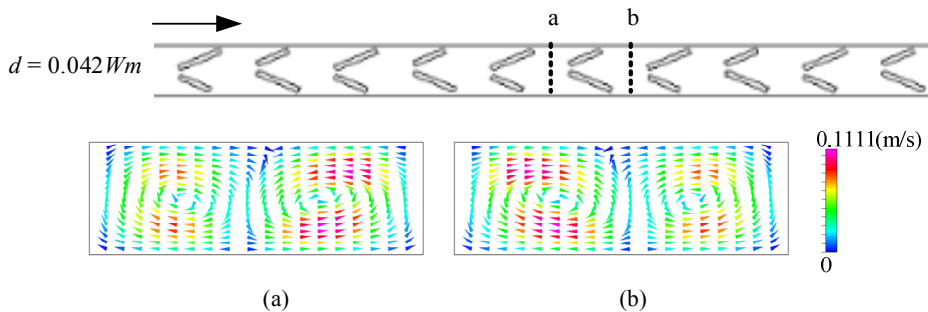


Fig. 5 Simulated flow patterns on vertical cross sections in the downstream zone of the RWP's with $\theta = 22.5^\circ$, $h = 0.75H$, $d = 0.042W_m$ and $D = 1.5W_m$ for the case with $Re = 64$

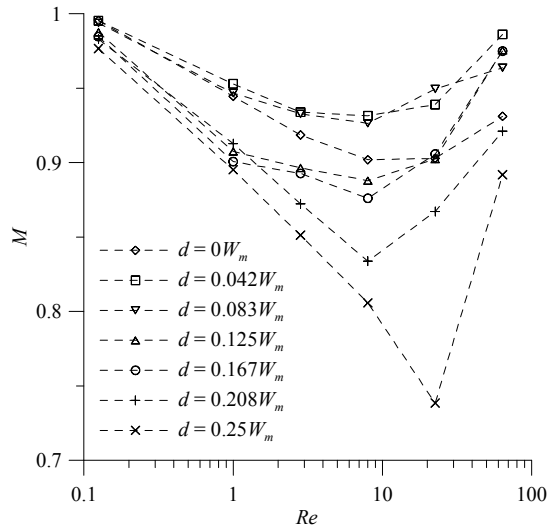


Fig. 6 Effect of asymmetry index on the degrees of mixing at the exit of the FTS micromixer with RWPs ($h = 0.75H, \theta = 22.5^\circ, D = 1.5W_m$) at $Re = 0.125, 1, 8, 64$

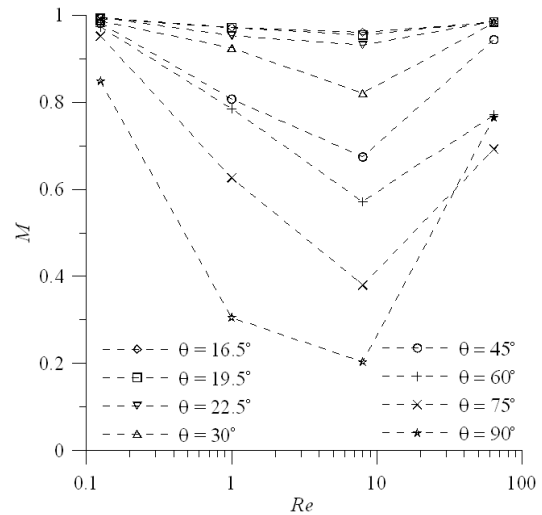


Fig. 8 Effect of angle of attack on the degrees of mixing at the exit of the FTS micromixer with RWPs ($h = 0.75H, d = 0.042W_m, D = 1.5W_m$) at $Re = 0.125, 1, 8, 64$

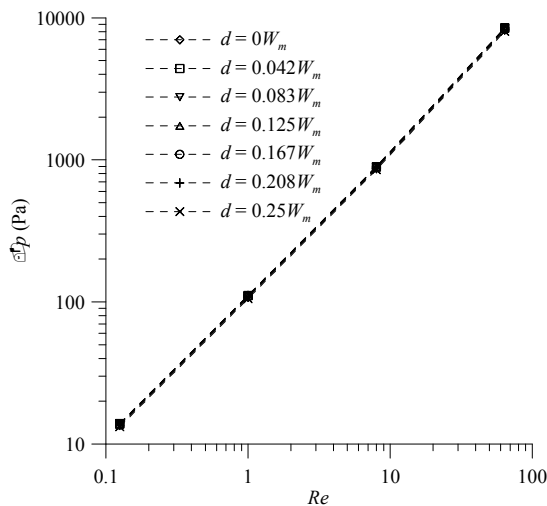


Fig. 7 Effect of asymmetry index on the pressures applied between the inlets and the exit of the FTS micromixer with RWPs ($h = 0.75H, \theta = 22.5^\circ, D = 1.5W_m$) at $Re = 0.125, 1, 8, 64$

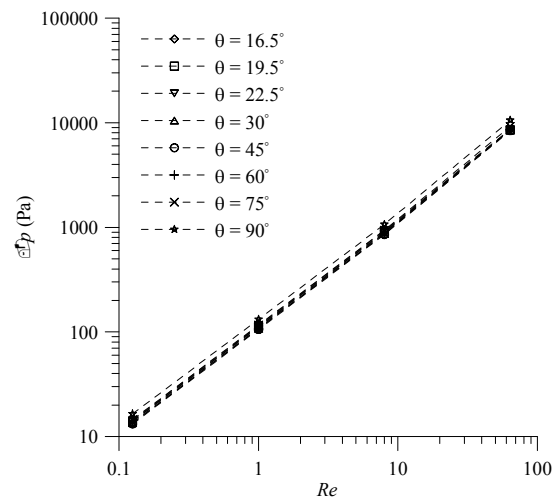


Fig. 9 Effect of angle of attack on the pressures applied between the inlets and the exit of the FTS micromixer with RWPs ($h = 0.75H, d = 0.042W_m, D = 1.5W_m$) at $Re = 0.125, 1, 8, 64$

Finally, we investigate the effects of the attack angle (θ) on fluid mixing. Fig. 8 shows that the micromixer using five mixing modules of the RWPs with $\theta = 16.5^\circ, 19.5^\circ$ or 22.5° can achieve excellent mixing ($M > 0.9$) over a wide range of Reynolds numbers. The pressure drop increases considerably as θ approaches 90° and the effects of θ on the pressure drop is small for $\theta \leq 45^\circ$, as shown in Fig. 9. Fig. 8 also shows that the degrees of mixing decreases with the increase of θ , except for the case with θ close to 90° at a relative larger Reynolds number ($Re = 64$). This is because the separation vortices with dominant transverse component are generated as the attack angle reaches 90° for the case with $Re = 64$. The transverse vortices have axes perpendicular to the main flow direction and induce a large pressure drop. Therefore, the RWPs with a small attack angle are more efficient than those with an attack angle close to 90° when pressure losses are taken into account.

VI. CONCLUDING REMARKS

In this work, we investigate the effects of the asymmetry index and the attack angle of RWPs built in a FTS channel on fluid mixing by numerical simulations. The numerical simulations are validated by comparing the numerical and experimental results. The following trends may be observed from the concentration distributions and flow patterns of the flow in the micromixers for various values of Re considered. (i) The micromixer with RWPs at a small asymmetry index is superior to the micromixer with symmetric RWPs and that with RWPs at a large asymmetry index. (ii) The micromixer using five mixing modules of the RWPs with $\theta = 16.5^\circ, 19.5^\circ$ or 22.5° can achieve excellent mixing ($M > 0.9$) over a wide range of Reynolds numbers. (iii) The micromixer with RWPs at a small attack angle is more efficient than that with a larger attack angle when pressure losses are taken into account.

ACKNOWLEDGMENT

This work is supported by the National Science Council of the Republic of China on Taiwan through Grant NSC 101-2221 - E - 006 - 108 - MY3. We appreciate the Center for Micro/Nano Science and Technology and the University Center for Bioscience and Biotechnology in National Cheng Kung University for the accesses of fabrication and experimental equipments.

REFERENCES

- [1] V. Hessel, H. Löwe, and F. Schönfeld, "Micromixers—a review on passive and active mixing principles," *Chem. Eng. Sci.*, vol. 60, pp. 2479-2501, 2005.
- [2] N. T. Nguyen and Z. Wu, "Micromixers—a review," *J. Micromech. Microeng.*, vol. 15, pp. R1-R16, 2005.
- [3] G. S. Jeong, S. Chung, C. B. Kim, and S. H. Lee, "Applications of micromixing technology," *Analyst*, vol. 135, pp. 460-473, 2010.
- [4] A. D. Stroock, S. K. W. Dertinger, A. Ajdari, I. Mezic, H. A. Stone, and G. M. Whitesides, "Chaotic mixer for microchannels," *Science*, vol. 295, pp. 647-651, 2002.
- [5] S. W. Lee, D. S. Kim, S. S. Lee, and T. H. Kwon, "A split and recombination micromixer fabricated in a PDMS three-dimensional structure," *J. Micromech. Microeng.*, vol. 16, pp. 1067-1072, 2006.
- [6] R. Yang, J. D. Williams, and W. J. Wang, "A rapid micro-mixer/reactor based on arrays of spatially impinging micro-jets," *J. Micromech. Microeng.*, vol. 14, pp. 1345-1351, 2004.
- [7] N. Aoki, R. Umei, A. Yoshida, and K. Mae, "Design method for micromixers considering influence of channel confluence and bend on diffusion length," *Chem. Eng. J.*, vol. 167, pp. 643-650, 2011.
- [8] M. Engler, N. Kockmann, T. Kiefer, and P. Woias, "Numerical and experimental investigations on liquid mixing in static micromixers," *Chem. Eng. J.*, vol. 101, pp. 315-322, 2004.
- [9] V. Hessel, S. Hardt, H. Löwe, and F. Schönfeld, "Laminar mixing in different interdigital micromixers: I. Experimental characterization," *AIChE J.*, vol. 49, pp. 566-577, 2003.
- [10] K. S. Drese, "Optimization of interdigital micromixers via analytical modeling - exemplified with the SuperFocus mixer," *Chem. Eng. J.*, vol. 101, pp. 403-407, 2004.
- [11] M. Q. Yi and H. H. Bau, "The kinematics of bend-induced mixing in micro-conduits," *Int. J. Heat Fluid Flow.*, vol. 24, pp. 645-656, 2003.
- [12] F. Jiang, K. S. Drese, S. Hardt, M. Küpper, and F. Schönfeld, "Helical flows and chaotic mixing in curved micro channels," *AIChE J.*, vol. 50, pp. 2297-2305, 2004.
- [13] R.-T. Tsai and C.-Y. Wu, "An efficient micromixer based on multidirectional vortices due to baffles and channel curvature," *Biomicrofluidics*, vol. 5, 2011.
- [14] C.-Y. Wu and R.-T. Tsai, "Fluid mixing via multidirectional vortices in converging-diverging meandering microchannels with semi-elliptical side walls," *Chem. Eng. J.*, vol. 217, pp. 320-328, 2013.
- [15] A. Bertsch, S. Heimgartner, P. Cousseau, and P. Renaud, "Static micromixers based on large-scale industrial mixer geometry," *Lab Chip*, vol. 1, pp. 56-60, 2001.
- [16] Y.-L. He and Y. Zhang, "Advances and outlooks of heat transfer enhancement by longitudinal vortex generators," in: *Advances in Heat Transfer*, vol. 44, E. M. Sparrow, Y. I. Cho, J. P. Abraham and J. M. Gorman, Eds. Amsterdam: Elsevier, 2012, pp. 119-185.
- [17] M. Kaniewski, H. W. Hahne, and N. K. Mitra, "Mass transfer enhancement by longitudinal vortices," *Heat and Mass Transf.*, vol. 32, pp. 163-166, 1997.
- [18] C. Liu, J.-T. Teng, J.-C. Chu, Y.-L. Chiu, S. Y. Huang, S. P. Jin, T. T. Dang, R. Greif, and H. H. Pan., "Experimental investigations on liquid flow and heat transfer in rectangular microchannel with longitudinal vortex generators," *Int. J. Heat Mass Transf.*, vol. 54, pp. 3069-3080, 2011.
- [19] K.-Y. Hsiao, C.-Y. Wu, and Y.-T. Huang, "Fluid mixing in a microchannel with longitudinal vortex generators," *Chem. Eng. J.*, vol. 235, pp. 27-36, 2014.
- [20] R.-T. Tsai and C.-Y. Wu, "Multidirectional vortices mixing in three-stream micromixers with two inlets," *Microsyst. Technol.*, vol. 18, pp. 779-786, 2012.
- [21] S. A. Rani, B. Pitts, and P. S. Stewart, "Rapid diffusion of fluorescent tracers into *Staphylococcus epidermidis* biofilms visualized by time lapse microscopy," *Antimicrob. Agents Chemother.*, vol. 49, pp. 728-732, 2005.
- [22] J. Boss, "Evaluation of the homogeneity degree of mixture," *Bulk Solids Handl.*, vol. 6, pp. 1207-1215, 1986.